UMYU Scientifica, Vol. 3 NO. 4, December 2024, Pp 232 – 243
https://doi.org/10.56919/usci.2434.018
ISSN: 2955 – 1145 (print); 2955 – 1153 (online)
*A periodical of the Faculty of Natural and Applied Sciences, UMYU, Katsina*

ORIGINAL RESEARCH ARTICLE

# Corrosion Inhibition and Adsorption Behaviour of *Centrosema pubescens* Leaf Extract for Copper in HCl Solution

Chikezie Ogueji[1] and Udochukwu Rita Ugwumba[1]
[1]Department of Chemistry, Alex Ekwueme Federal University, Ndufu-Alike, P. M. B. 1010 Abakiliki, Ebonyi State, Nigeria

**ARTICLE HISTORY**
Received July 11, 2024
Accepted October 25, 2024
Published October 30, 2024

**KEYWORDS**
Inhibitor, Weight loss, Copper, Adsorption isotherm

**ABSTRACT**
The anti-corrosion behaviour of *Centrosema pubescens* leaf extract (CPE) on copper in 1.5 M hydrochloric acid was investigated using weight loss method at different temperatures, followed with scanning electron microscopy (SEM) surface characterization connected with energy dispersive X-ray spectroscopy (EDX). The Fourier transform infrared spectrum of CPE was obtained. CPE inhibition effectiveness depends on the temperature and its concentration. CPE restrains the copper corrosion with 94.26 % inhibition efficiency at 1.0 g/L of CPE and at 303 K. For the CPE-inhibited system, a higher activation energy (Ea) value (range of 31.09 to 38.70 kJmol$^{-1}$) compared to 20.34 kJmol$^{-1}$ of the blank solution was obtained. The reaction process is spontaneous and endo thermic, as indicated by the ΔH, ΔS and ΔG values calculated. CPE adsorption behaviour fitted best into Freundlich isotherm.



## INTRODUCTION

Metals deteriorate or oxidize as a result of chemical interaction with their environment. This is referred to as corrosion (Mobin et al., 2020; Ani et al., 2022; Hossain et al., 2023). One of the industrial practices is the cleaning of industrial equipment, which involves the use of acids and it has its resultant effects on the metal (Hemapriya et al., 2021). Copper corrodes when exposed to aggressive media (Fateh et al., 2017). One crucial technique is the use of inhibitors to control the menace of metal deterioration (Onwu et al., 2016; Şahin, 2022).

Different classes of compounds have been applied and confirmed to be good corrosion inhibitors. However, the majority of these corrosion inhibitors present management issues due to their cost, toxicity, ease of supply, and environmental friendliness (Ogueji et al., 2024; Eddy and Ameh, 2021). Organic inhibitors have been recognised as effective inhibitors (Mazumder et al., 2022), and their adsorption on a metal surface relies on the electronic structure of the molecule (Guruprasada et al., 2020; Alaoui et al., 2020). From studies, organic inhibitors with heteroatoms, have been recognized as the main adsorption sites (Hemapriya et al., 2021). Some of the reported effective organic inhibitors include 3-((5-mercapto-1,3,4- thiadiazol-2-yl) imino)indolin-2-one ( Gu et al., 2023; Betti et al., 2023; Ogueji et al., 2024), clotrimazole (Ade et al., 2014; Guruprasada et al., 2020), benzothiazines (Hemapriya et al., 2019), atenolol (Atheel et al., 2017; Ogueji et al., 2024), N,N'-bis-(1-hydroxyphenylimine)-2,5-thiophenedicarboxaldehyde (Wanees and Seda, 2019; Ogueji et al., 2024), etc. However, these organic inhibitors are expensive, toxic, and incompatible with human health and the environment, and this has led to a real search for alternatives.

The need and interest in green inhibitors have increased because they are eco-friendly. Plant extracts (leaves, roots, seed and stems), impressively, have shown to be the reliable needed alternative to their organic counterparts (Ofuyekpone et al., 2021). The biomolecules present in the plant extract contain electronegative atoms (N, O, S, P, etc.) and unsaturated bonds. The inhibitory potential of many plants extracts in HCl solutions has been reported (Ofuyekpone et al., 2021), such as *Justicia secunda* (Iroha and Maduelosi, 2021), *Carica papaya* (Nwigwe, 2019), garlic extracts (Loto and Loto, 2016), *Eruca sativa* (Singh et al., 2015; Nwigwe et al., 2023), *Chamaerops humilis* (Fekkar et al., 2020; Nwigwe et al., 2023; Wang et al., 2023), *Rhizophora Apiculata* (Asaad et al., 2017; Nwigwe et al., 2023), *Allium cepa* (Aiboudi et al., 2019, Nwigwe et al., 2023), *Eruca sativa* (Alrafai, 2022), *Beta vulgaris* (Joycee, 2022), *Jatropha Curcas* (Ajayi et al., 2014). Ofuyekpone et al. (2021), reported the prevention of mild steel corrosion by Centrosema pubescens leaf extract in $H_2SO_4$ medium.

Centrosema pubescens, or butterfly pea, as commonly called, belongs to the family Fabaceae; it has climbing, twinning, and herbaceous stem (Ofuyekpone et al., 2021). *Centrosema pubescens* leaves extract (CPE) has not been

**Correspondence:** Chikezie Ogueji. Department of Chemistry, Alex Ekwueme Federal University, Ndufu-Alike, P. M. B. 1010 Abakiliki, Ebonyi State, Nigeria. ✉ ogueji.chikezie@funai.edu.ng.
**How to cite**: Ogueji, C., & Ugwumba, U. R. (2024). Corrosion Inhibition and Adsorption Behaviour of *Centrosema pubescens* Leaf Extract for Copper in HCl Solution. *UMYU Scientifica*, 3(4), 232 – 243. https://doi.org/10.56919/usci.2434.018

examined or documented for inhibiting copper corrosion in any media. Regarding the current study, FT-IR spectroscopy, SEM surface characterization connected with EDX, and weight loss investigations of copper corrosion in 1.5 M HCl solution at various CPE concentrations were conducted.

## MATERIALS AND METHODS

### Materials

A rectangular specimen of pure copper was employed for this work. It was mechanically press-cut into coupons measuring 3 cm x 1 cm x 0.12 cm. The gravimetric investigation employed a 1.5 M $HCl_{(aq)}$.

Fresh matured leaves of *Centrocema pubescens* were harvested in Abakiliki, Ebonyi State, Nigeria, and were identified by a botanist.

The leaves were washed and shade-dried for seven days to constant weight, blended and immersed in ethanol for 48 hours, then filtered. The filtrates were exposed to evaporation using a rotary evaporator at 40 $^{o}$C until all solvents had been eliminated. The extract was dried in a desiccator and preserved. Inhibitor test solutions were prepared with the *Centrocema pubescens* leaf extract (CPE) at concentrations of 0.2 g $L^{-1}$, 0.4 g $L^{-1}$, 0.6 g $L^{-1}$, 0.8 g $L^{-1}$, and 1.0 g $L^{-1}$ for use in the corrosion inhibition tests. To do this, 0.05 g, 0.10 g, 0.15 g, 0.2 g, and 0.25 g of CPE were added to 250 mL of 1.5 M HCl solution in a flask.

### Gravimetric method

The gravimetric test was carried out as documented elsewhere (Ekuma et al., 2017; Ogueji et al., 2023; Ogueji et al., 2024). In order to perform the gravimetric measurement, the previously weighed coupons were submerged in 100 mL of the test solution (1.5 M HCl) in six different beakers that contained varying amounts of CPE at 303 K in a thermostatic water bath (0.0 g/L, 0.2 g/L to 1.0 g/L). When the two-hour exposure period was finished, the coupon was taken out of the solution, cleaned to halt the corrosion reaction, rinsed in water, dried in acetone, and then reweighed using an analytical weighing scale. At 313, 323, and 333 K, the same procedure was carried out once more. The experiment was redone at 303 K, and the metal was taken out every hour for five hours. Weight loss, surface coverage, corrosion rate, and inhibitory efficiency were calculated using equations 1, 2, 3, and 4 (Ogueji et al., 2024).

$$\Delta W = W_1 - W_2 \quad (1)$$

$$\theta = \frac{CR_{un} - CR_{in}}{CR_{un}} \quad (2)$$

$$\text{Corrosion rate} = \Delta W / At \quad (3)$$

$$I.E\% = \frac{CR_{un} - CR_{in}}{CR_{un}} \, x \, 100 \quad (4)$$

### Characterisation

The CPE was analyzed using FTIR spectrum obtained in the range of 400 to 4000 $cm^{-1}$. The surface characteristics of the copper coupons were captured using (SEM) (JEOL-Model JSM - 6360) fitted with (EDX) (model JED-2300) (Hemapriya *et al.*, 2021; Nwigwe et al., 2023; Ogueji et al., 2024).

## RESULTS AND DISCUSSION

### FTIR analysis

The unique bands that correlate to the functional groups found in CPE's active components can be seen in the FT-IR spectrum (Figure 1).

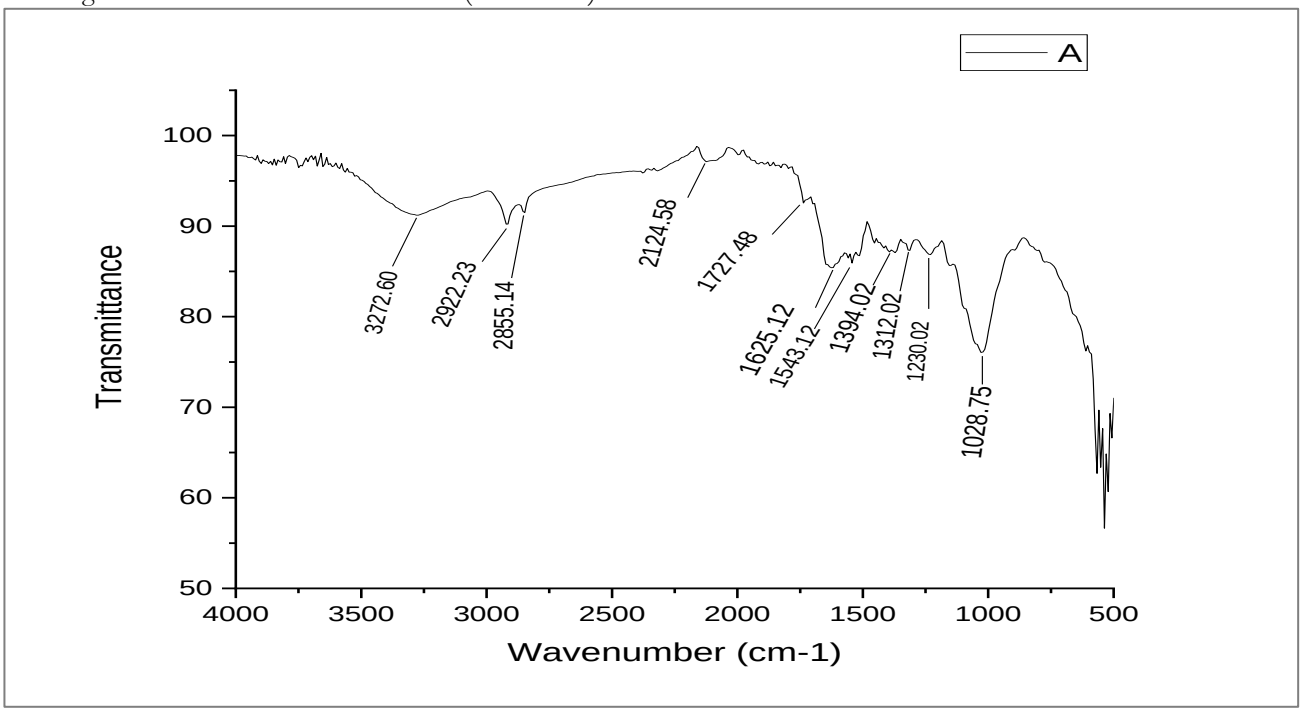


**Figure 1: FTIR spectrum of CPE**

The active components' phenolic, carboxylic acid and aromatic amino groups were linked to the absorption band at 3272.60 cm−1, which resulted from −OH stretching overlapped with a N–H stretching mode (Hemapriya *et al.*, 2021; Fouda *et al.*, 2016b). The bands at 2922.60 $cm^{-1}$, 1727.48 $cm^{-1}$, and 1625.12 $cm^{-1}$ emerged from C–H stretching vibrations, C=N and C=O stretching vibrations, respectively. Other functional groups in the spectrum are C=C (1543.12 $cm^{-1}$), C-H (1394.02 $cm^{-1}$), C=N (1230.02 $cm^{-1}$), C-O (1028.75 $cm^{-1}$) and C-N (1312.02 $cm^{-1}$).

Alkaloids, proteins, flavonoids, organic pigments, tannins, organic and amino acids (Umoren et al., 2016), and their acid hydrolysis products are among the phytochemicals present in Centrosema pubescens leaf extract, according to Ofuyekpone et al. (2021). These phytochemicals have been shown to be beneficial against acid corrosion.

**Effect of inhibitor concentration and temperature**

The inhibition of copper corrosion in 1.5 M HCl containing 0.0 g/L, 0.2 g $L^{-1}$ to 1.0 g $L^{-1}$ of CPE at different temperatures for 2 h was examined employing the weight loss approach. Figure 2 and Figure 3 show plots for the variation of corrosion rate with temperature and inhibition efficiency with temperature, respectively, for the degradation of copper in 1.5 M HCl solution in 0.0 g/L, 0.2 to 1.0 g/L of CPE. The effectiveness of inhibition of CPE in 1.5 M HCl is presented in Table 1.

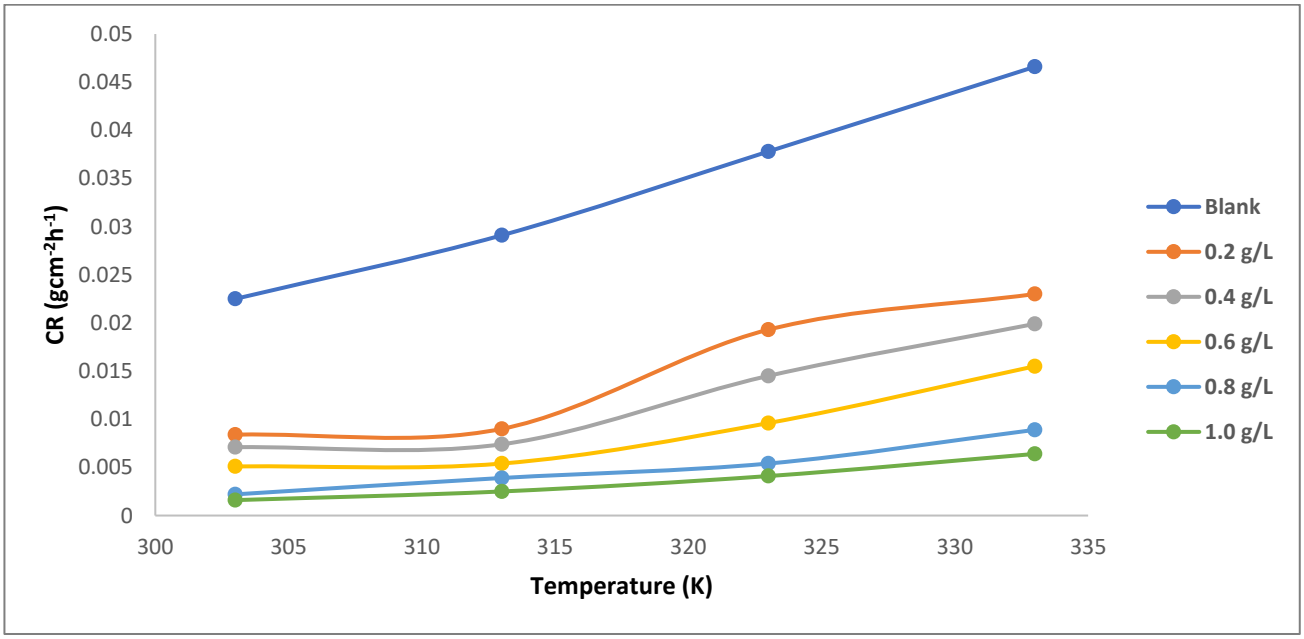


**Figure2: Variation of corrosion rate of Cu with temperature in 1.5 M of HCl containing various concentrations of CPE**

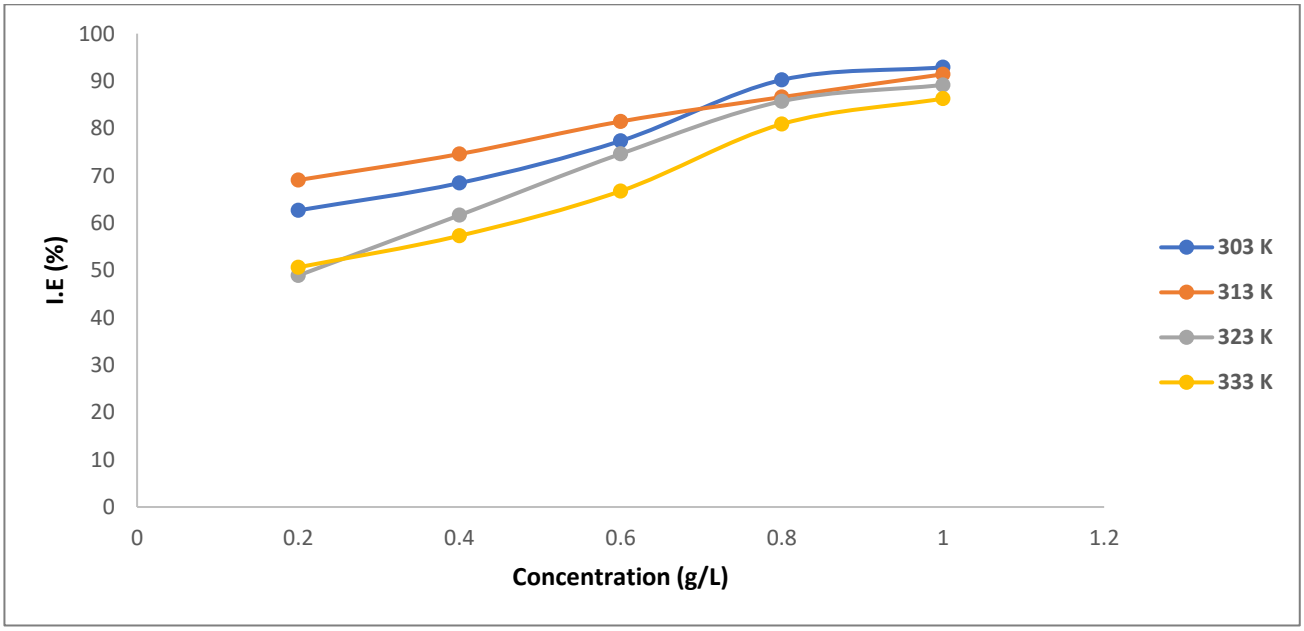


**Figure 3: Variation of inhibition efficiency with concentrations of CPE in 1.5 M of HCl**

Figure 2 revealed that the blank specimens recorded the highest corrosion rate of copper compared to the results for solutions with different CPE concentrations. The graphs also demonstrate a consistent decline in copper corrosion rate with rising CPE concentration and a rise in copper corrosion rate with rising temperature. This suggests that CPE retarded the corrosion of copper in HCl. This was a result of the interaction between the heteroatoms in the phytochemicals available in CPE and the copper (Eddy and Ameh, 2021).

**Table 1: Inhibition efficiency (%) of CPE in 1.5 M HCl**

| | 303 K | 313 K | 323 K | 333 K |
|---|---|---|---|---|
| Conc. (g/L) | I.E (%) | I.E (%) | I.E (%) | I.E (%) |
| 0.2 | 62.67 | 69.07 | 48.9 | 50.64 |
| 0.4 | 68.44 | 74.57 | 61.64 | 57.30 |
| 0.6 | 77.33 | 81.44 | 74.60 | 66.74 |
| 0.8 | 90.22 | 86.60 | 85.71 | 80.90 |
| 1.0 | 92.89 | 91.41 | 89.15 | 86.27 |

As observed from Figure 3 and Table 1, while the inhibitory efficacy of CPE reduced with rising temperatures, it rose as CPE concentration increased. The highest possible inhibition efficiency of 92.89 % was attained at 303K with a CPE concentration of 1.0 g/L. The CPE's inhibitory effectiveness value decreases with temperature, indicating that physical adsorption may play a role in the process (Ikeuba and Okafor, 2019).

### Effect of Immersion Time

Figure 4 and Figure 5 show plots for the variation of corrosion rate with time and inhibition efficiency with time, respectively, for copper corrosion in 1.5 M HCl solution in 0.0 g/L, 0.2 -1.0 g $L^{-1}$ of CPE. The corrosion rate dropped as the CPE concentration increased, but it progressively increased as the contact period increased, as seen in Figure 4. Similarly, with variation of contact time, as the concentration of CPE rose, the inhibitory efficiency steadily decreased, as shown in Figure 5 and Table 2. With 1.0 g/L CPE concentration and a 1-hour immersion period at 303K, a maximum inhibitory efficiency of 94.26% was attained. Table 2 shows the inhibitory efficacy of CPE at various contact times at 303K.

**Table 2: Inhibition efficiency (%) of CPE in 1.5 M HCl at different contact time**

| | 0.2 g/L | 0.4 g/L | 0.6 g/L | 0.8 g/L | 1.0 g/L |
|---|---|---|---|---|---|
| Time | I.E (%) | I.E (%) | I.E (%) | I.E (%) | I.E (%) |
| 1 hr | 65.55 | 71.29 | 80.38 | 92.34 | 94.26 |
| 2 hrs | 62.67 | 68.44 | 77.33 | 90.22 | 92.89 |
| 3 hrs | 60.49 | 66.67 | 76.54 | 88.48 | 91.36 |
| 4 hrs | 55.40 | 62.59 | 72.30 | 85.25 | 88.85 |
| 5 hrs | 52.24 | 71.88 | 67.53 | 75.53 | 82.35 |

The unobstructed active sites at the copper/acid interface on the copper surface are where corrosion happens; the CPE molecules' adsorption may block these sites (Hemapriya *et al.*, 2021; Onwu et al., 2016). The movement of CPE molecules from the bulk electrolyte onto the copper surface, whereupon they were adsorbed as a thin layer to shield the metal from the corrosive environment (Hemapriya *et al.*, 2021), was the reason for the drop in corrosion rate and rise in inhibition efficiency (Rathore et al., 2023; Hemapriya *et al.*, 2021; Eddy and Ameh, 2021; Ofuyekpone et al., 2021; Ekuma et al., 2017; Wadhwani et al., 2015). The current CPE exhibits a higher inhibitory efficacy in comparison to numerous other inhibitors, such as Chamaerops humilis L. extract (88.0%) (Fekkar et al., 2020); Tapinanthus bangwensis leaf extract (76.87 %), (Eddy and Ameh, 2021); *Azadirachta Indica* leaf extract (72.03), (Nwigwe *et al.*, 2023); *Santolina chamaecyparissus* extract (86.9 %) (Shabani-Nooshabadi and Ghandchi, 2015); *Newbouldialaevis* extracts (77.53 %), (Okeoma *et al.*, 2016), etc.

### Surface study by SEM and EDX analysis

Following a two-hour soak in 1.5 M HCl in 0.0 g/L, 0.2 – 1.0 g/L of CPE, the appearance of the surface of the copper coupon was examined using SEM-EDX. The SEM-EDX images are displayed in Figures 6 and 7.

Clearly, a damaged surface with signs of pits, cavities, and/or cracks is seen in Figure 6(a), which only confirms that copper dissolves in an acidic media (Ofuyekpone *et al.*, 2021; Guruprasad *et al.*, 2020). But after CPE was introduced as an inhibitor (Figure 7a), it displayed a reduced level of damage, which indicates the development of a coating that is both protective and inhibitive on the copper surface (Hemapriya et al., 2020; Ofuyekpone *et al.*, 2021; Yadav et al., 2023; Ogueji et al., 2023).

Precisely, an EDX spectrum identifies the principal component elements at the surface of the metal coupon. The EDX of the spectrum in Figure 6(b) and Figure 7(b) identifies high peaks of the important element, which further helped to verify that the metal is copper (Ofuyekpone *et al.*, 2021). The copper specimen that has corroded in a blank 1.5 M HCl solution is seen in the EDX spectrum of Figure 6(b), which is attached. The measured copper (Cu) atomic concentration was approximately 75.85% in the blank system; however, after adding CPE (Figure 7b), Cu atomic content was greatly reduced to 72.27 % (Table 3) due to adsorption on the surface. The development of an inhibitive film on the coupon is the cause of the muted Cu lines (Ofuyekpone *et al.*, 2021).

### Adsorption consideration

Equation (5), which reduces to equation (6), may be employed to explain the study of CPE adsorption on copper surfaces using the Langmuir adsorption isotherm model (Ekuma et al., 2017; Salman et al., 2019;

Guruprasad et al., 2021; Ogueji et al., 2023; Njoku et al., 2023).

$$\frac{C}{\theta} = {}^{1}/_{K_{ads}} + C \quad (5)$$

$$\text{Log}\left(\frac{C}{\theta}\right) = \log C - \log K_{ads} \quad (6)$$

The Langmuir adsorption isotherms for CPE adsorption on the surfaces of copper are displayed in Figure 8. $K_{ads}$ can be determined from the intercept.

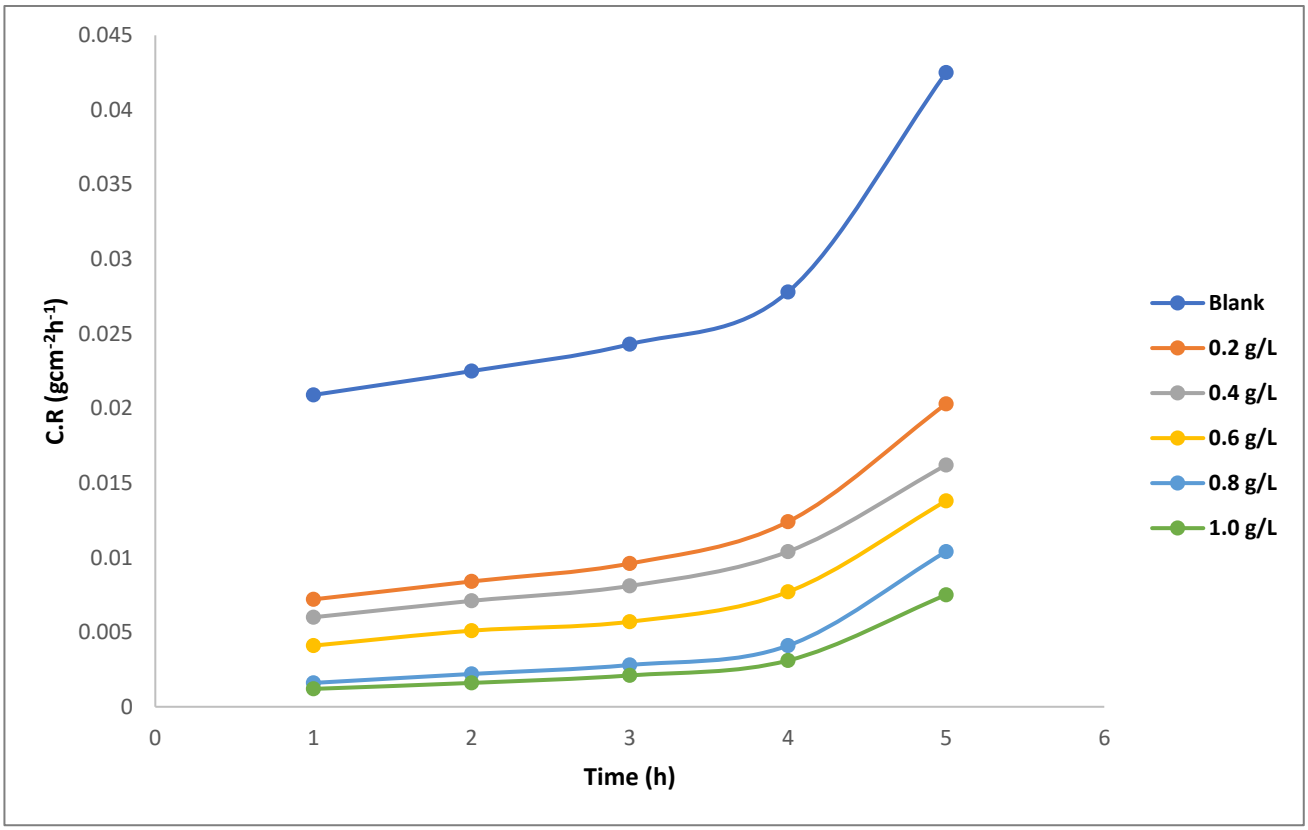


**Figure 4: Variation of corrosion rate of Cu with time in 1.5 M of HCl containing various concentrations of CPE**

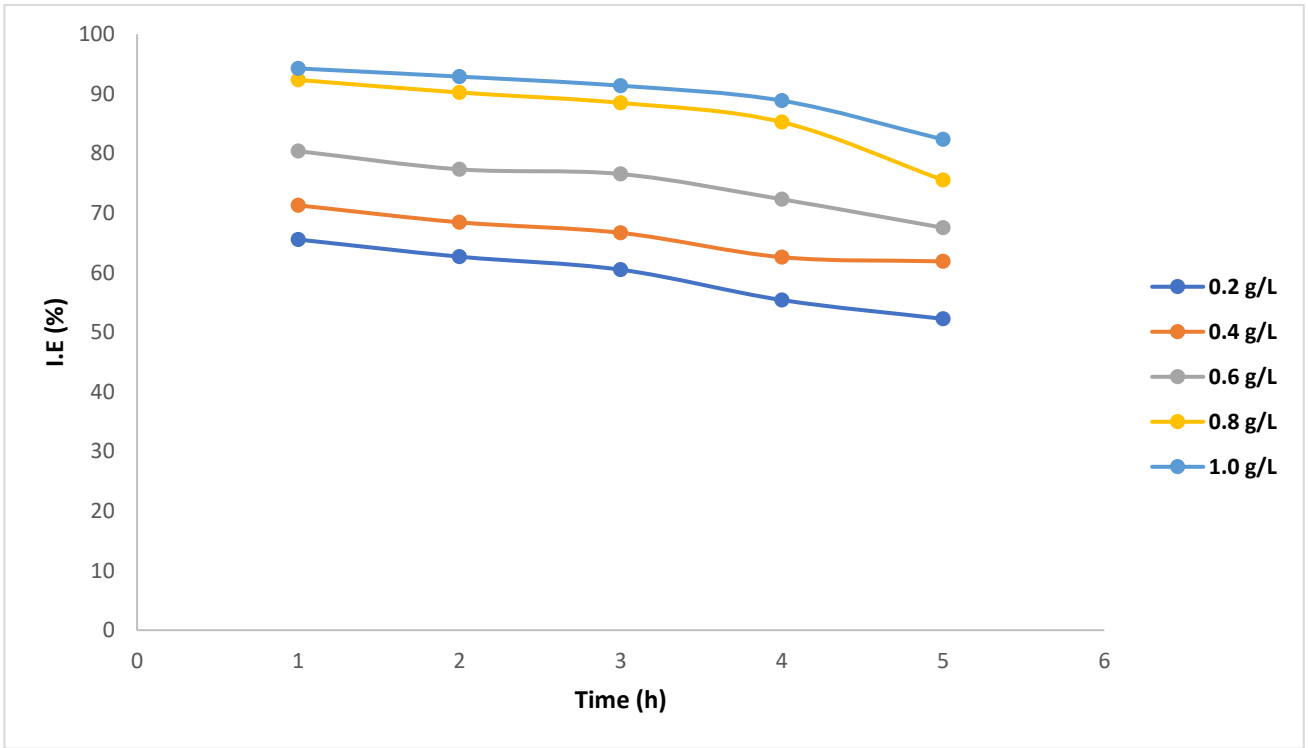


**Figure 5: Variation of inhibition efficiency of CPE with time in 1.5 M of HCl**

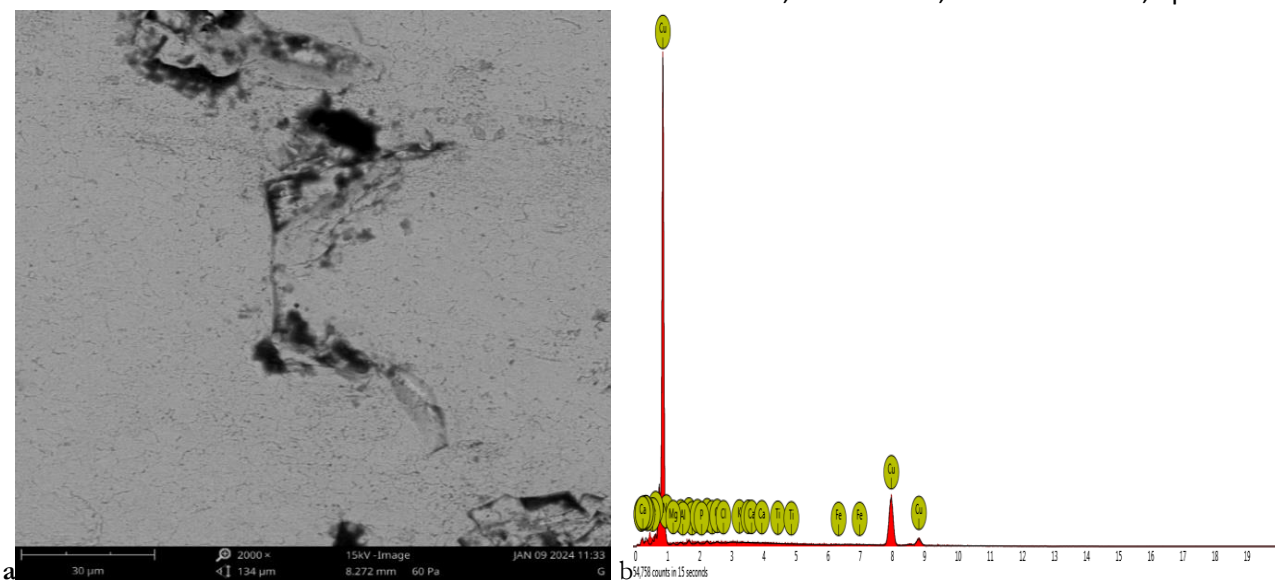


**Figure 6: SEM-EDX images of copper in 1.5 M HCl in 0.0 g/L of CPE**

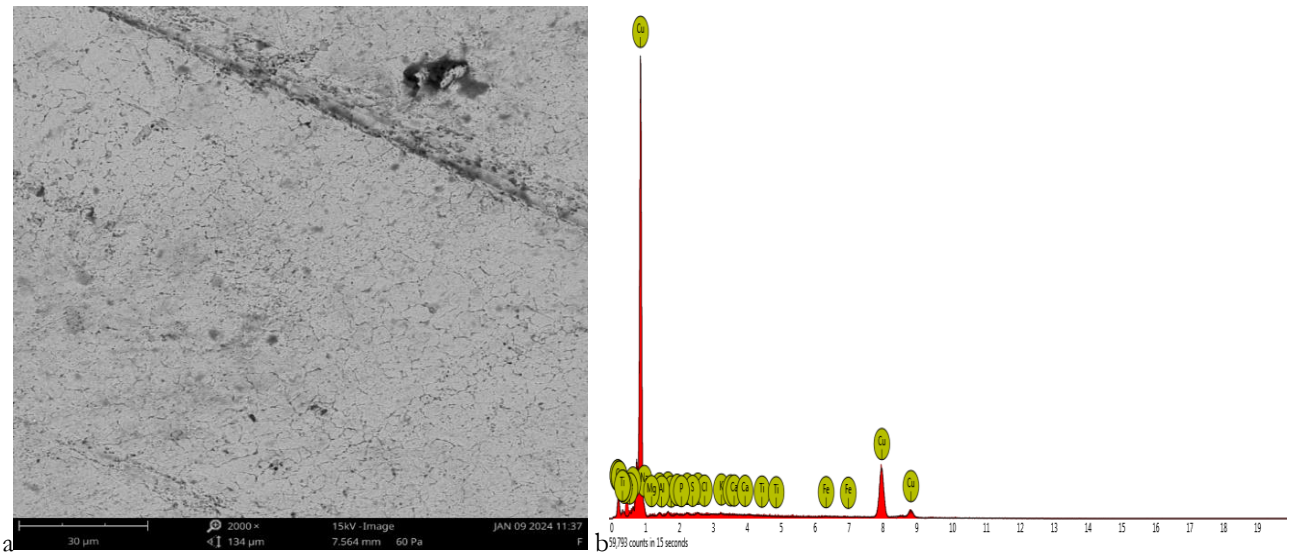


**Figure7: SEM-EDX images of copper in 1.5 M HCl with CPE**

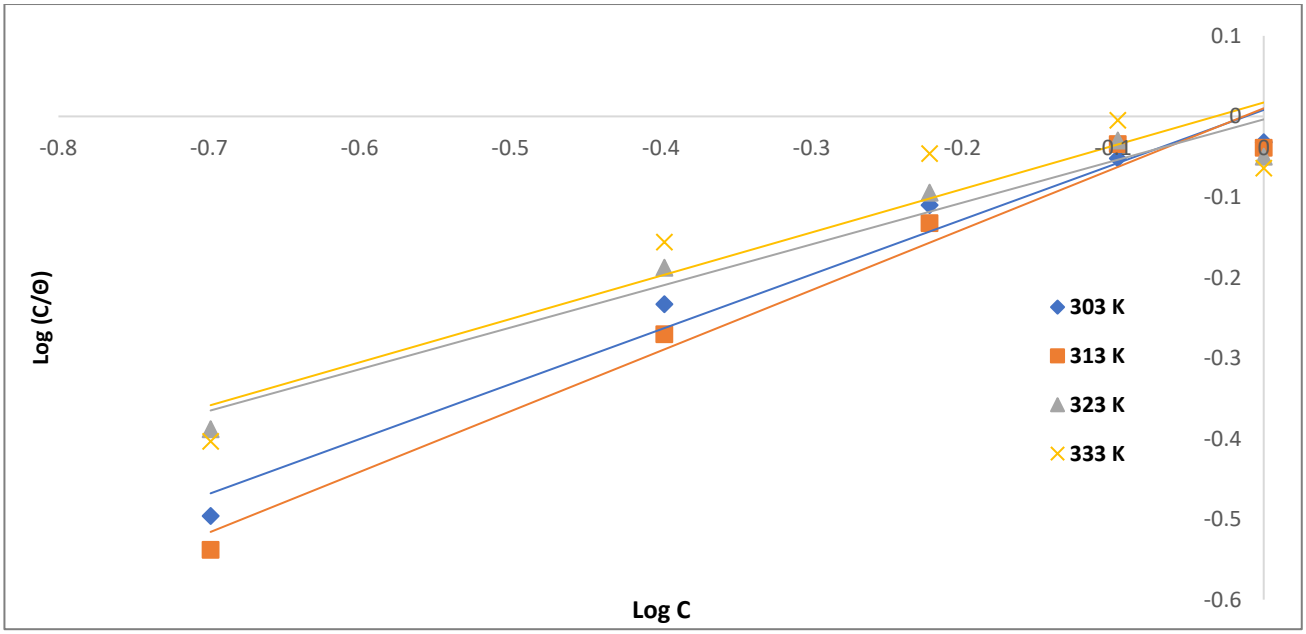


**Figure 8: Langmuir plots for the adsorption of CPE**

**Table 3: % of elements' atomic composition as determined by EDX spectroscopy**

| System | Cu | Na | Si | Mg | AI | S | P | Cl | Fe | K |
|---|---|---|---|---|---|---|---|---|---|---|
| Immersed in 1.5M HCl Solution | 75.85 | 17.17 | 1.59 | 1.73 | 1.17 | 0.95 | 0.90 | 0.52 | 0.12 | 0.00 |
| Immersed in 1.5M HCl with CPE | 72.27 | 21.11 | 1.51 | 1.07 | 1.56 | 0.65 | 0.61 | 0.69 | 0.23 | 0.32 |

Table 4 displays the values of the Langmuir adsorption isotherm parameters that were obtained from the plots. The findings indicate that the slopes are not precisely equal to one; the $R^2$ values obtained ranged from 0.8602 to 0.9739, and these results indicate that the $R^2$ values for the plots are nearly one except for the value obtained at 333K, which indicates that the experimental data may not have adhered strongly to the assumptions of Langmuir (Eddy and Ameh, 2021; Ofuyekpone et al., 2021).

**Table 4: The parameters of Langmuir for CPE adsorption onto the surface**

| Temperature (K) | $R^2$ | $K_{ads}$ | Slope |
|---|---|---|---|
| 303 | 0.9699 | 1.0188 | 0.6811 |
| 313 | 0.9739 | 1.0235 | 0.7524 |
| 323 | 0.9501 | 1.0086 | 0.517 |
| 333 | 0.8602 | 1.0404 | 0.5376 |

The Freundlich isotherm is based on multilayer adsorption on heterogeneous surfaces. Freundlich equation and its linear form are expressed as in equations (7) and (8), respectively.

$$\Theta = KC^{1/n} \quad (7)$$

$$\text{Log } \Theta = \log K + \frac{1}{n} \log C \quad (8)$$

From the linear plot of log θ against log C, the values of n and K are ascertained (Ogunleye et al., 2019). The Freundlich plots are displayed in Figure 9, and the Freundlich isotherm parameters are also provided in Table 5.

From Figure 9 and Table 5, the values of $R^2$ for the adsorption of CPE onto copper surface ranged from 0.9336 to 0.9914, showing that the experimental data fitted best into the Freundlich compared to Langmuir isotherm model. It was reported (Onwu *et al.*, 2016) that when the n value is within 1< n <10, it is a favourable uptake process, and the n values from the current study ranged from 2.5628 to 5.7176, and this implies that the adsorption process is favourable. Utilization of Freundlich isotherm to the uptake of CPE on copper reveals that the mode of the adsorption process may have involved a physisorption based on multilayer, as confirmed by Freundlich (Onwu *et al.*, 2016).

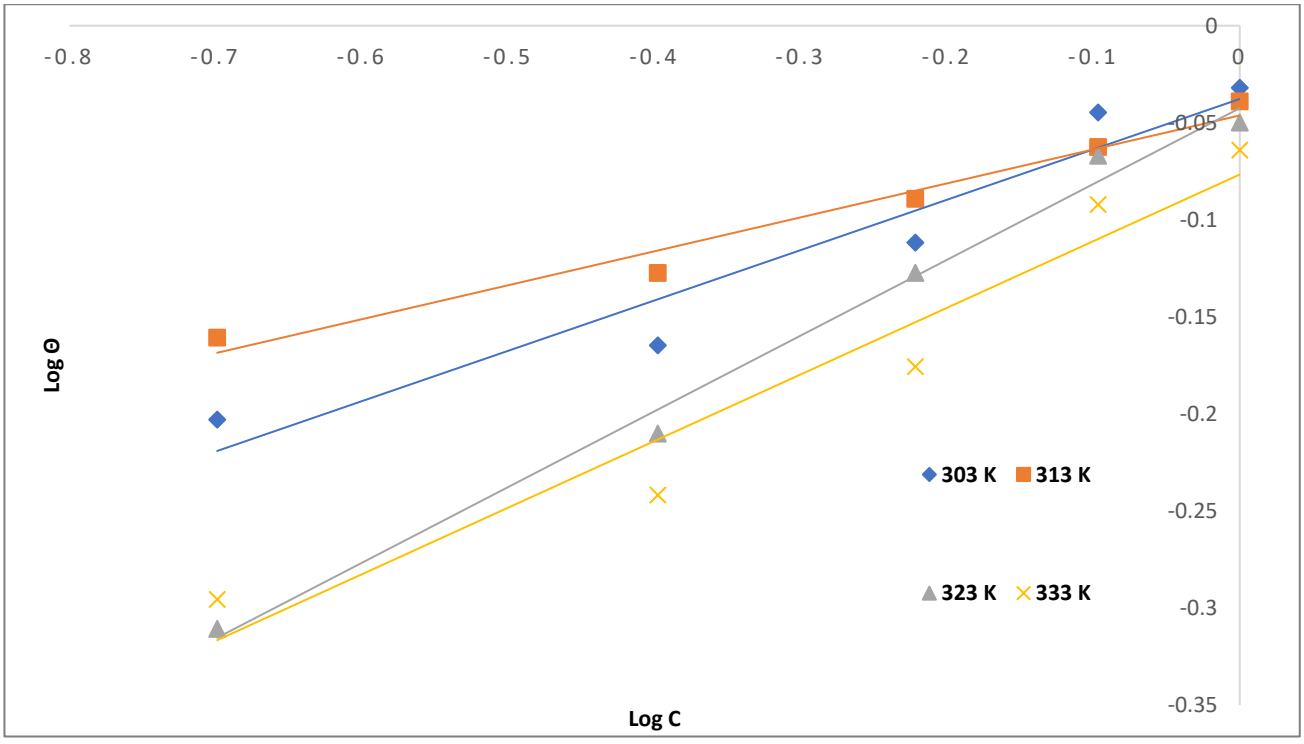


**Figure 9: Freundlich isotherm for the adsorption of CPE at different temperatures**

**Table 5: Freundlich isotherm parameters for CPE adsorption onto the surface**

| Temperature (K) | K | n | $R^2$ |
|---|---|---|---|
| 303 | 0.9166 | 3.8551 | 0.9336 |
| 313 | 1.1122 | 5.7176 | 0 .9724 |
| 323 | 1.1028 | 2.5628 | 0.9914 |
| 333 | 0.8381 | 2.9138 | 0.9409 |

**Thermodynamics consideration**

The corrosion response of a copper coupon in 1.5 M HCl, both without and with CPE, can be better understood by calculating the activation energy (Ea), enthalpy (ΔH), and entropy (ΔS) (Jmiai et al., 2018). The Arrhenius equations (9), the transition state equation (10), and equation (11) were utilized to calculate these parameters using the Arrhenius plots and transition state plots (Wanees et al., 2017).

$$Log\ CR = logA - {}^{Ea}/_{2.303\ RT} \quad (9)$$

$$Log\left(\frac{CR}{T}\right) = log\frac{R}{Nh} + \frac{\Delta S}{2.303R} - {}^{\Delta H}/_{2.303RT} \quad (10)$$

$$\Delta G = \Delta H - T\Delta S \quad (11)$$

Figure 10 shows the Arrhenius plot for the corrosion inhibition of copper in 1.5 M of HCl in 0.2 – 1.0 g/L of CPE. The values of Ea obtained from the graphs are provided in Table 6.

An enormous range of values, from 20.34 to 38.70 kJ/mol, was obtained for the activation energies. The Ea values obtained for the inhibited corrosion reaction of copper (from 31.31 to 38.70 kJ/mol) are greater than the 20.34 kJ/mol obtained for the uncontrolled. This indicates that copper corrosion was retarded by varied concentrations of CPE (Wanees et al., 2017, 2019; Ekuma *et al.*, 2017).

The transition state graph was done by plotting log (CR/T) against 1/T (Equation 10), which gives a straight line (Onwu et al., 2016; Ogueji et al., 2024). From which the slope is - ΔH/2.303R, while the intercept is log R/Nh + ΔS/2.303R, and ΔG was determined from equation (11) (Aslam et al., 2017; Ogueji et al., 2023; Ogueji et al., 2024). Figure 11 shows the Transition state plots for the inhibition of copper in 1.5 M of HCl in various concentrations of CPE. The values of entropy (ΔS), enthalpy (ΔH), and free energy (ΔG) obtained from the graphs are presented in Table 6.

Table 6 displays positive computed values of ΔH, showing endothermic adsorption of the inhibitor on the copper surface (Ekuma et al., 2017; Lai et al., 2017). CPE-controlled processes showed greater ΔH values, indicating a higher energy barrier for the reaction in the presence of the inhibitor (Rbaa *et al.*, 2017; Ouakki *et al.*, 2018; Mzioud et al., 2022). The data revealed that the entropy of activation, ΔS, for the uninhibited reaction was higher than the inhibited; this implies a decrease in the degree of disorderliness in the presence of CPE (Todres, 2019; Echchibi et al., 2019; Lahbib et al., 2020; Nahlé *et al.*, 2021).

The values of ΔG obtained ranged from –56.2 to -63.53 kJ/mol, -41.3 to -48.17 kJ/mol, -40.8 to -47.61 kJ/mol, -40.0 to -46.88 kJ/mol, -40.48 to -45.30 kH/mol and -39.67 to – 44.51 kJ/mol at CPE concentrations of 0.0, 0.2, 0.4, 0.6, 0.8 and 1.0 g/L respectively. A spontaneous uptake process is indicated by negative values of ΔG (Dkhireche *et al.*, 2018). According to the findings, the free energies are greater than the threshold value of -40 kJ/mol required for chemical adsorption (Ameh, 2012; Abdel-Hameed et al., 2022) in the various concentrations of CPE at all temperatures, except in 0.8 g/L and 1.0 g/L of CPE at 303 K where the values are lower than -40 kJ/mol (Nahlé *et al.*, 2021; Ogueji et al., 2023).

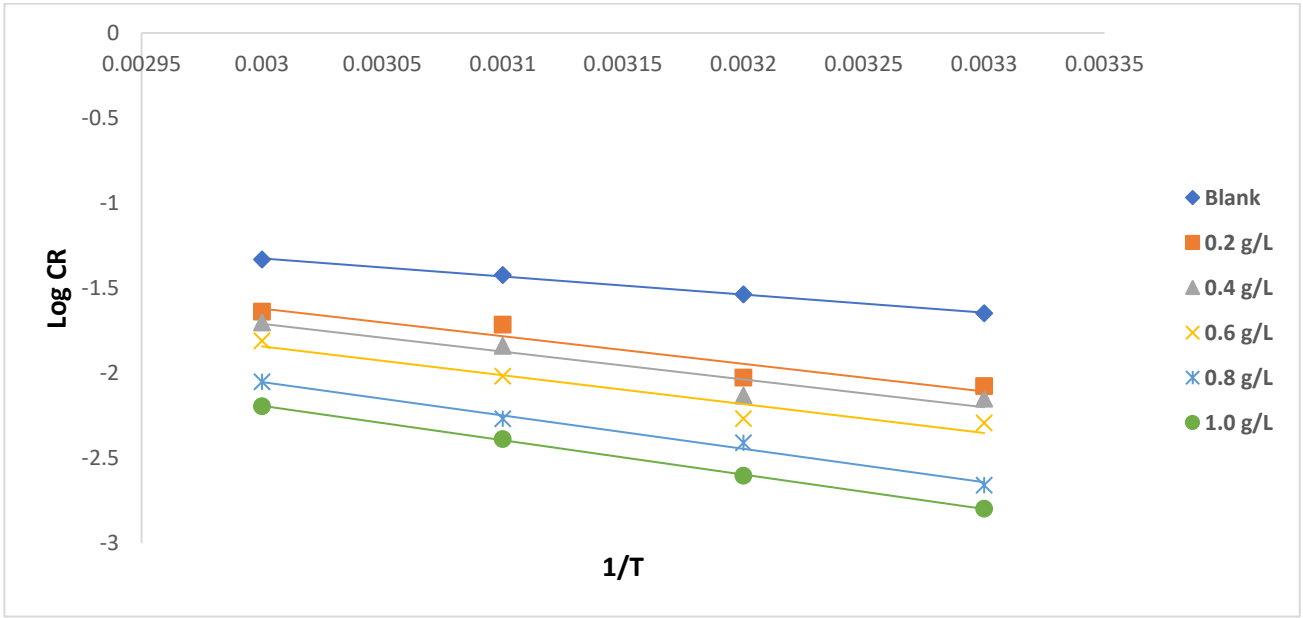


**Figure 10: Arrhenius plot for the inhibition of copper corrosion in 1.5 M of HCl in CPE**

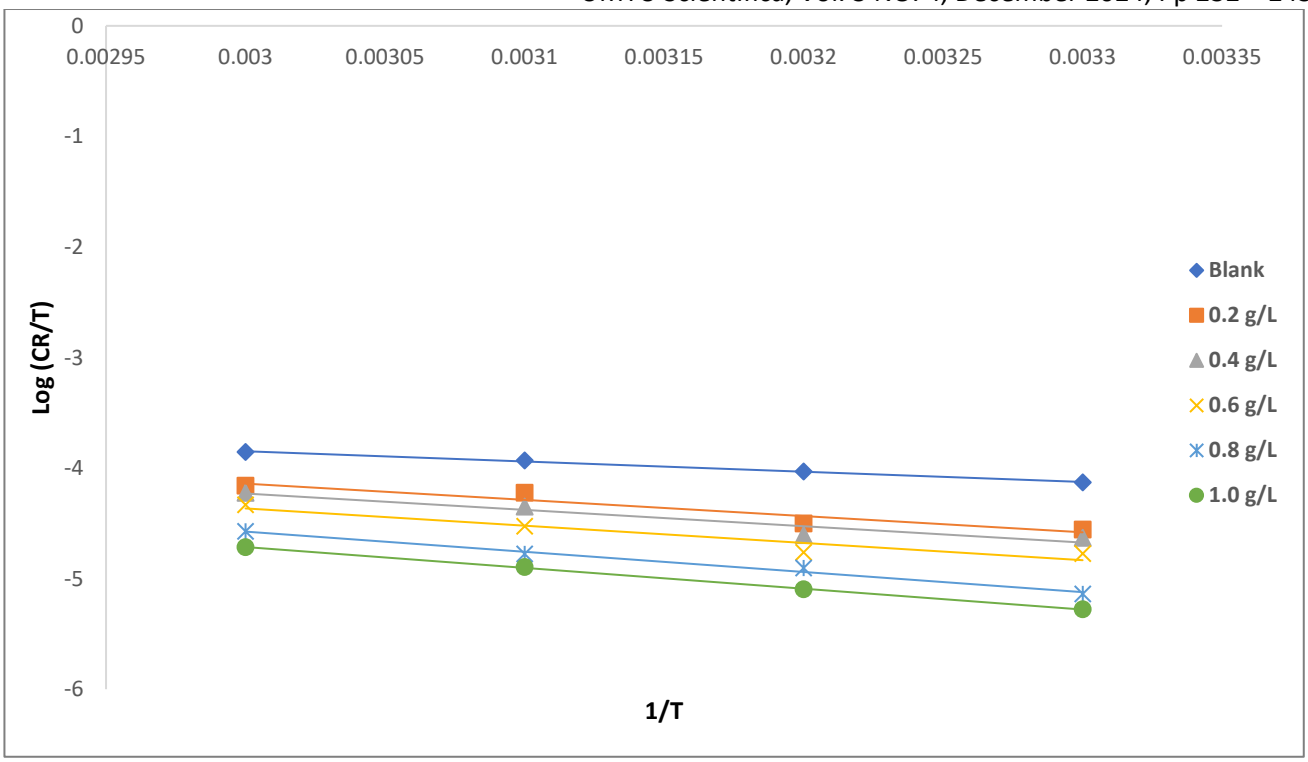


**Figure 11: Transition state plots for the inhibition of copper in 1.5 M of HCl in various concentrations of CPE**

**Table 6: Thermodynamic values for CPE uptake onto copper surface in (kJ/mol)**

| Conc. (g/L) | $E_a$ | ΔH | ΔS | ΔG 303 K | ΔG 313 K | ΔG 323 K | ΔG 333 K |
|---|---|---|---|---|---|---|---|
| 0.0 | 20.34 | 17.72 | 0.2444 | -56.2 | -58.65 | -61.09 | -63.53 |
| 0.2 | 31.09 | 28.09 | 0.229 | -41.3 | -43.59 | -45.89 | -48.17 |
| 0.4 | 31.31 | 28.31 | 0.228 | -40.8 | -43.06 | -45.33 | -47.61 |
| 0.6 | 32.49 | 29.71 | 0.230 | -40.0 | -42.28 | -44.58 | -46.88 |
| 0.8 | 37.57 | 34.95 | 0.241 | -38.1 | -40.48 | -42.89 | -45.30 |
| 1.0 | 38.70 | 36.08 | 0.242 | -37.2 | -39.67 | -42.09 | -44.51 |

## CONCLUSION

From the results and findings of the study, we conclude that CPE is effective at preventing the corrosion of copper in HCl. CPE inhibited copper corrosion with a maximum inhibition efficiency of 94.26 % at 30 ° C and at the maximum inhibitor concentration of 1.0 g/L. The corrosion rate of copper in HCl is dependent on temperature and inhibitor concentration. The positive values of enthalpy revealed that the uptake of CPE onto copper surface is endothermic. The negative values of ΔG showed that the processes were feasible and spontaneous. The adsorption isotherm data fitted best into the Freundlich isotherm model (indicating multilayer coverage) as compared to Langmuir with a correlation coefficient ($R^2$) of 0.9914. The thermodynamic parameter, ΔG of the reaction, and the adsorption isotherm data suggest both chemisorption and physisorption mechanisms. CPE can be applied as an effective corrosion inhibitor by researchers against metallic corrosion.

## RECOMMENDATIONS

It is recommended that further research should be made using other conventional methods, with the same inhibitor and compare the results and findings.

## AUTHORS' CONTRIBUTIONS

Dr. Chikezie Ogueji developed the research plan supervised, and analysed the data. Udochukwu Rita Ugwumba did the practical work and wrote part of the manuscript.

## DECLARATION OF COMPETING INTEREST

None.

## REFERENCES

Abdelsattar, M., Badawi, A. M., Ibrahim, S., Wasfy, A. F., Tantawy, A. H., Dardir, M. M., "Corrosion Control of Carbon Steel in WaterBased Mud by Nanosized Metallo-Cationic Surfactant Complexes During Drilling Operations", ACS Omega, 5 (2020), 30881-30897. **[Crossref]**

Abdel-Hameed, R., Qureshi, M.T., Abdallah, M., Aljuhani E., Alzharani, A. A., Alfarsi, A., Bakry, A. M.,

Huwaimel, B. & Farghaly, O., "Recycling of Expired Lactulose Drugs as Eco-Friendly Corrosion Inhibitor for Steel Alloys in Acidic Environment: Gravimetrical and Electrochemical Studies", International Journal of Electrochemical Science, 17 (2022) 221270. **[Crossref]**

Ade, S.B., Shitole, N.V., & Lonkar S.M., Antifungal drug's used as metal corrosion inhibitor in various acid medium, *Int. J. Chem Tech. Res.* 6 (7) (2014), 3642–3650.

Aiboudi M., Yousfi, F., Fekkar, G., Bouyazza, L., Ramdani, M., El Azzouzi, M. & Abdel- Rahman, I., Eco-friendly Allium cepa L. seeds extracts as corrosion inhibitor for mild steel in 1 M HCl solutions. *J. Mater. Environ. Sci.*, 10(4) (2019), pp. 339–346.

Ajayi, O., Odusote, J., & Yahya, R., Inhibition of mild steel corrosion using Jatropha Curcas leaf extract. *J. Electrochemical Sci Eng.*, 4(2) (2014), pp. 67–74. **[Crossref]**

Alaoui, K., Dkhireche, N., Touhami, M. E. & El Kacimi, Y., "chapter 5 Review of Application of Imidazole and Imidazole Derivatives as Corrosion Inhibitors of Metals", IGI Global, 2020. **[Crossref]**

Alrafai, H., Corrosion inhibition properties of the oil extracted from the leaves of Eruca sativa for carbon steel in acidic medium. *Int J Electrochem Sci.*, 17(2022), pp. 1–12. **[Crossref]**

Ameh, P. O., "Corrosion inhibition and adsorption behaviour for mild steel by Ficus glumosa gum in H2SO4 solution", African Journal of Pure and Applied Chemistry, 6 (7) (2012), 100-106. **[Crossref]**

Ani, J.U., Obi, I.O., Akpomie, K.G., Eze, S.I. & Nwatu, G., Corrosion Inhibition Studies of Metals in Acid Media by Fibrous Plant Biomass Extracts and Density Functional Theory: A Mini-Review, *Journal of Natural Fibers* 19 (7) (2022), 2391–2401, **[Crossref]**

Asaad M. A., Ismail, M., Raja, P. B. & Khalid, N. A., Rhizophora Apiculata as Eco-Friendly Inhibitor Against Mild Steel Corrosion in 1M HCl. *Surf Rev Lett.*, 24(8) (2017), pp. 1–11. **[Crossref]**

Aslam, R., Mobin, M., Zehra, S., Obot, I.B. & Ebenso, E.E., Dialkylcystine Gemini and Monomeric - Alkyl Cysteine Surfactants as Corrosion Inhibitors on Mild Steel Corrosion in 1 M HCl Solution: A Comparative Study, *ACS Omega*, 2(9) (2017), **[Crossref]**

Atheel, H.A, Dhuha, H.F., Ali, A.A., Abdul Hameed, F. & Yousif, E., Inhibitive effect of atenolol on the corrosion of zinc in hydrochloric acid, *Rasayan J. Chem.* 10 (3) (2017) 922–928.

Betti, N., Al-Amiery, A., KhalidAl-Azzawi, W. & Isahak, W, N., Corrosion inhibition properties of schif base derivative against mild steel in HCl environment complemented with DFT investigations. *Nature Scientifc Reports* (2023) 13:8979. **[Crossref]**

Dkhireche, N., Galai, M., El Kacimi, Y., Rbaa, M., Ouakki, M., Lakhrissi, B. & EbnTouhami, M., New quinoline derivatives as sulfuric acid inhibitor's for mild steel. *Anal Bioanal Electrochem* 10(1) (2018):111–135

Eddy, N.O. & Ameh, P.O., Computational and experimental study on Tapinanthus bangwensis leaves as corrosion inhibitor for mild steel and Al in 0.1 M HCl. *Current Topics in Electrochemistry* Vol. 23, 2021.

Ech-chihbi, E., Nahlé, A., Salim, R., Oudda H., "An Investigation into Quantum Chemistry and Experimental Evaluation of Imidazopyridine Derivatives as Corrosion Inhibitors for C-Steel in Acidic Media", Journal of Bio- and Tribo-Corrosion, (2019). **[Crossref]**

Ekuma, F.K., Ogueji, C. & Okoyeagu, A. Zinc corrosion inhibition by 4-hydroxyl phenyl methylidene-2-(1-phenyl ethylidene) hydrazine carbothioamide (4-HPMHC) and 4-hydroxy phenyl [methylidene] amino-3, 4- dimethyl-5-phenyl cyclo pent-2-en-1- one (4-HPMCP), *J. Chem. Soc. Nigeria,* 42(2) (2017), 5-10.

Fateh, A., Aliofkhazraei, M. & Rezvanian, A. R., Review of Corrosive Environments for Copper and its Corrosion Inhibitors. *Arabian Journal of Chemistry*, (2017), **[Crossref]**

Fekkar, G., Yousfi, F., Elmsellem, H., Aiboudi, M., Ramdani, M., Abdel-Rahman, I., Hammouti, B., & Bouyazza, L., Eco-friendly chamaerops humilis l. Fruit extract corrosion inhibitor for mild steel in 1 M HCl. *International Journal of Corrosion and Scale Inhibition*, 9(2) (2020), pp. 446–459. **[Crossref]**.

Gu, T., Xu, Z., Zheng, X., Fu, A., Zhang, F., Al-Zaqri, N., Chen, J., Tan, B., & Li, W. (2023). "Lycium barbarum leaf extract as biodegradable corrosion inhibitor for copper in sulfuric acid medium", *Industrial Crops and Products*. **[Crossref]**

Guruprasada, A.M., Sachinb, H.P., Swethab, G.A. & Prasannad, B.M., Corrosion inhibition of zinc in 0.1 M hydrochloric acid medium with clotrimazole: Experimental, theoretical and quantum studies. *Surfaces and Interfaces*, 19 (2020) 100478. **[Crossref]**

Hemapriya, V., Chung, I. M., Parameswari, K., Chitra, S., Kim, S. H., & Prabakaran, M. Corrosion inhibition behavior of benzothiazine derivative on low carbon steel in acid medium: adsorption and quantum chemical investigations, *Surf. Rev. Lett.* 26 (10) (2019)., 1950066. **[Crossref]**

Hemapriya, V., Prabakaran, M., Chitra, S., Swathika, M., Chung, S. I., "Utilization of biowaste as an eco-friendly 1% biodegradable corrosion inhibitor for mild steel in 1mol/L HCl solution", Arabian Journal of Chemistry, 13 (12) (2020), 8684-8696. **[Crossref]**

Hemapriya,V., Chung, I., Kim, S. & Prabakaran, M., Inhibitory effect of biowaste on copper corrosion in 1 M HCl solution, *Materials Today Communications,* 27(2021), **[Crossref]**

Hossain N., Islam, M. A. & Chowdhury, M. A., Advances of plant-extracted inhibitors in metal corrosion reduction – Future prospects and challenges. *Results in Chemistry*, 5 (2023). **[Crossref]**

Ikeuba, A.I. & Okafor, P.C., Green corrosion protection for mild steel in acidic media: saponins and crude extracts of Gongronema latifolium. Pigment & Resin Technology, 48(1) (2019):57-64. **[Crossref]**

Iroha, N. & Maduelosi, N.,'Corrosion Inhibitive Action and Adsorption Behaviour of Justicia Secunda Leaves Extract as an Eco-friendly Inhibitor for Aluminium in Acidic Media', *Biointerface Res Appl Chem*., 11(5), pp. 13019–13030. **[Crossref]**

Joycee, S., Corrosion mitigation by an eco-friendly inhibitor: Beta vulgaris (beetroot) extract on mild steel in simulated oil well water medium. *Int J Corros Scale Inhib*., 11(1) (2022), pp. 82–101. **[Crossref]**

Lahbib, H., Hassen, S. B., Gerengi, H., Amor, Y. B.," Inhibition effect of Cynara cardunculus leaf extract on corrosion of St37 steel immersed in seawater with and without bleach solution ", Chemical Engineering Communications, (2020). **[Crossref]**

Lai, C., Xie, B., Zou, L., Zheng, X. & Ma, X., Adsorption and Corrosion Inhibition of Mild Steel in Hydrochloric Acid Solution by S-allyl-O,O'-dialkyldithiophosphates, 7(2017). **[Crossref]**

Loto, C. & Loto, R., Inhibition effect of garlic extracts on the corrosion of alpha brass in nitric acid. Der Pharma Chem., 8(2) (2016); pp. 162–171.

Mahmoud, G. A., Saleh, S., Wanees, A., Mustafa, S. K.,"Dihydropyridine derivatives as controllers for production of hydrogen during zinc dissolution". Chemical Engineering Communications, 206 (6) (2019)., 789-803. **[Crossref]**

Mazumder, M. J., Quraishi, M. & Ahmed, A. (2022)."Polymeric Corrosion Inhibitors for Greening the Chemical and Petrochemical Industry", Wiley, 2022. **[Crossref]**

Mobin, M., Ahmad, I., Basik, M., Murmu, M. & Banerjee, P., "Experimental and theoretical assessment of almond gum as an economically and environmentally viable corrosion inhibitor for mild steel in 1M HCl", Sustainable Chemistry and Pharmacy, 18 (2020), 100337. **[Crossref]**

Mobin, M., & Rizvi, M., Inhibitory effect of xanthan gum and synergistic surfactant additives for mild steel corrosion in 1M HCl. *Carbohydr Polym*., 136(2016), pp. 384–393. **[Crossref]**

Mzioud, K., Habsaoui, A., Rached, S., Lachhab, R., "Chapter 23 Synergistic Effect from Allium Sativum Essential Oil and Diethylthiourea for Corrosion Inhibition of Carbon Steel in 0.5 MH2SO4 Medium", Springer Science and Business Media LLC, (2022). **[Crossref]**

Nahlé, A., El Azzouzi, M., Aouniti, A., Abrigach, F., Djedouani, A., Benhiba, F., Touzani, R., Warad, I., Obot, I.B., Zarrouk, A., Hammouti, B., Experimental, Quantum Chemical and Monte Carlo Simulation Studies on the Corrosion Inhibition of Mild Steel by Three New Schiff Base Derivatives. *Portugaliae Electrochimica Acta* 39(2021), 293-321. **[Crossref]**

Njoku, C. N., Enendu, B. N., Okechukwu, S. J., Igboko, N., "Review on anti- corrosion properties of expired antihypertensive drugs as benign corrosion inhibitors for metallic materials in various environments", Results in Engineering, 18 (2023), 101183. **[Crossref]**

Nwigwe, U., The inhibition of Carica papaya leaves extract on the corrosion of cold worked and annealed mild steel in HCl and NaOH solutions using a weight loss technique. *Eng Appl Sci Research*, 46(2019), pp. 114– 119. **[Crossref]**.

Nwigwe, U. S., Nwoye, C. I., Bello, A. S. & Nwankwo, N. E., Azadirachta Indica's adsorptive behavior on mild steel in a sulfuric acid medium. *UNIZIK Journal of Engineering and Applied Sciences,* 2(2) (2023), 319-331.

Ofuyekpone, O.D., Utub, O.G. & Onyekp, B.O., Corrosion inhibition for alloy 304L (UNS S30403) in H2SO4 1M solution by Centrosema pubescens leaves extract. Applied Surface Science Advances, 3(2021) 100061. **[Crossref]**

Ogueji, C., Amadi, O. K., Oranuka, D. C., & Onwuka, C. A., Adsorption and inhibitive effect of N-[(4{[(Z)-(4-hydroxy phenyl) methylidene] amino} phenyl) sulfonyl acetamide on the corrosion of mild steel in HCl medium. UMYU Scientifica, 2(4) (2023), 179 – 188. **[Crossref]**

Ogueji, C., Mbah, M. C., Amadi, O. K., Okoro, L. N. & Okoli, C. P., Adsorption and thermodynamic study of the inhibition of corrosion of zinc in HCl medium using N- [(4{[(Z)-phenylmethylidene]amino}phenyl)sulfonyl] acetamide. UNIZIK Journal of Engineering and Applied Sciences 3(1) (2024), 416-429.

Ogunleye, O. O., Arinkoola, A. O., Alagbe, S. O., Agbede, O. O., Omodele, A. E., Morakinyo, A. F., Osho, Y. A., "Synthesis of green corrosion inhibitor for mild steel in acidic environment", Indian Chemical Engineer, (2019). **[Crossref]**

Okeoma, K.B., Mejeha, I.M. & Akajiaku, S.C., Investigative studies on the inhibitive effects of Newbouldialaevis extracts and magnetic fields on copper corrosion in aqueous acidic media. Research Inventy: International Journal of Engineering And Science,6(2) (2016), 5-14.

Onwu, F.K., Ogueji, C. & Mgbemena, N.M., Inhibition of Corrosion of Zinc in $H_2SO_4$ Medium by the Schiff Base, 4-Hydroxy Phenyl Methylidene-2-(l-Phenyl Ethylidene) Hydrazine Carbothioamide

(4-HPMHC), *DerChemica Sinica*, 7(4) (2016), 13-20.

Ouakki, M., Galai, M., Cherkaoui, M., Rif, E. & Hatim, Z., Inorganic compound (Apatite doped by Mg and Na) as a corrosion inhibitor for mild steel in phosphoric acidic medium. *Anal Bioanal Electrochem*, 10(7) (2018):943–960.

Rathore, A., Sharma, S., Sharma, A., Sharma, S. K. "Evaluation of structure-reactivity correlation of efficient corrosion inhibitor ionic liquids for mild steel in acidic medium", *Journal of Dispersion Science and Technology,* 2023. **[Crossref]**

Rbaa, M., Galai, M., El Kacimi, Y., Ouakki, M., Touir, R., Lakhrissi, B. & EbnTouhami, M., Adsorption properties and inhibition of carbon steel corrosion in a hydrochloric solution by 2-(4,5-diphenyl-4,5-dihydro-1h-imidazol-2-yl)-5 methoxyphenol, *Portugaliae. Electrochim Acta,* 35(6) (2017):323–338. **[Crossref]**

Şahin, E. A., "Experimental and theoretical studies of acridine orange as corrosion inhibitor for copper protection in acidic media", *Journal of the Indian Chemical Society*, 99(3) (2022), 100358. **[Crossref]**

Salman, T. et al., Novel ecofriendly corrosion inhibition of mild steel in strong acid environment: Adsorption studies and thermal effects. Int J Corros Scale Inhib., 8(4) (2019), pp. 1123–1137. **[Crossref]**

Shabani-Nooshabadi, M. & Ghandchi, M.S., Santolina chamaecyparissus extract as a natural source inhibitor for 304 stainless steel corrosion in 3.5% NaCl, *J. Ind. Eng. Chem.* 31(2015), 231–237. **[Crossref]**

Singh, A., Lin, Y., Ebenso, E. E., Liu, W., Pan, J. & Huang, B., Gingko biloba fruit extract as an eco-friendly corrosion inhibitor for J55 steel in CO2 saturated 3.5% NaCl solution. J Ind Eng Chem., 24(2015), pp. 219–228. **[Crossref]**

Todres, Z.V. (2019). "Chalcogenadiazoles Chemistry and Applications", CRC Press, 2019

Umoren, S.A., Eduok, U.M., Solomon, M.M., Udoh, A.P.,"Corrosion inhibition by leaves and stem extracts of Sida acuta for mild steel in 1M H2SO4 solutions investigated by chemical and spectroscopic techniques", Arabian Journal of Chemistry, 9 (2016), 5209-5224. **[Crossref]**

Wadhwani, P. M, Panchal, V. K, Shah, N. K., "Newly synthesized salicylidene-4,4'-dimorpholine (SDM) assembled on nickel oxide nanoparticles (NiONPs) and its inhibitive effect on mild steel in 2N hydrochloric acid", Applied Surface Science, 2015. **[Crossref]**

Wang, J., Cui, L., Chen, B., Chen, X., Lv, Z., Chen, D., Qiang, Y., Xiang, T., "Corrosion inhibition effect of Sycamore leaf extract on copper in H2SO4 solution", Journal of Materials Research and Technology, 26 (2023), 6689-6702. **[Crossref]**

Wanees, A. S., Radwan, A. B., Alsharif, M. A. & Abd El Haleem, S. M., Initiation and Inhibition of Pitting Corrosion on Reinforcing Steel under Natural Corrosion Conditions. Mater. Chem. Phys. 2017, 190, 79–95. **[Crossref]**

Wanees, S.A., & Seda, S. H., Corrosion inhibition of zinc in aqueous acidic media using a novel synthesized Schiff base – an experimental and theoretical study. *Journal of Dispersion Science and Technology*, (2019). **[Crossref]**

Yadav, S., Kaushik, S., Dheer, N., Kumar, S., SIngh, G., Chaudhary, M., Gupta, M., (2023). "Experimental investigation of anti-corrosive behaviour of Beta vulgaris: A green approach", Journal of Applied and Natural Science, 2023. **[Crossref]**